

LASERS

PACS numbers: 42.55.Wd; 42.60.Lh; 42.65.Ky
DOI: 10.1070/QE2013v043n05ABEH015032

Ytterbium-doped fibre laser tunable in the range 1017–1040 nm with second-harmonic generation*

E.I. Dontsova, S.I. Kablukov, S.A. Babin

Abstract. **A cladding-pumped ytterbium-doped fibre laser has been tuned to shorter emission wavelengths (from 1040 to 1017 nm). The laser output power obtained has been compared to calculation results. We have studied frequency doubling of the laser in a $KTiOPO_4$ (KTP) crystal with type II phase matching in the *XY* plane and demonstrated wavelength tuning in the range 510–520 nm.**

Keywords: *ytterbium-doped fibre laser, wavelength tuning, second-harmonic generation, KTP crystal.*

1. Introduction

Ytterbium-doped fibre lasers are used in various fields of science and technology owing to their small dimensions, high output power and output stability, in combination with the possibility of continuous emission wavelength tuning. Typical gain media of such lasers are double-clad optical fibres with an ytterbium-doped core. The laser transitions of the ytterbium ion are, as a rule, excited by 915- or 976-nm radiation of laser diodes. Efficient lasing near 1.1 μm can be achieved through cladding pumping of active fibre. At typical transverse fibre dimensions (core diameter, 4.5–5.5 μm; inner-cladding diameter, 120 μm), such lasers are most efficient in the spectral range 1060–1130 nm [1, 2]. Shorter wavelength lasing is impeded by resonance reabsorption, so the slope efficiency of ytterbium fibre lasers reaches 80% in the range 1080–1110 nm and drops to 57% at 1049 nm. Fibre Bragg gratings (FBGs) are used as reflectors in all-fibre cavities.

To tune a laser to shorter emission wavelengths, one should not only change the resonance wavelength of the FBG but also reduce the length of the gain medium, but the latter is accompanied by a reduction in laser efficiency. This is caused by the large difference in diameter between the core and inner cladding of the fibre, so that not all the pump power is absorbed in short fibres. In standard fibres, the cladding to core diameter ratio is 21–24. It is commonly reduced to improve the laser efficiency, but special diodes with high emission intensity are then needed. Reducing the inner-cladding diameter to 30 μm (so that the cladding to core diameter ratio was 3.6), optimising the output Bragg grating and utilising a special phosphosilicate active fibre, Kurkov et al. [3] obtained lasing at 1020 nm with 65% efficiency.

Light sources tunable in the blue-green spectral region are of great interest for scientific and biomedical applications. Such tuning can be ensured by a frequency-doubled fibre laser. Kablukov et al. [4] have demonstrated efficient lasing at 515 nm (argon laser line) using an ytterbium-doped fibre laser and frequency doubling in a $KTiOPO_4$ (KTP) crystal.

The purpose of this work was to examine the possibility of simultaneous tuning and frequency doubling of Yb^{3+}-doped fibre laser radiation in a KTP crystal in order to obtain a light source tunable in the blue-green spectral region (under 520 nm).

2. Experimental

In our experiments, we used a tunable ytterbium fibre laser cladding-pumped by several laser diodes in a configuration similar to that reported by Kablukov et al. [4] (Fig. 1).

The gain medium of the laser was a double-clad optical fibre with an Yb^{3+}-doped core. Multimode radiation from two pump laser diodes (LDs) was coupled into the inner cladding of the fibre using a pump combiner (PC). Propagating along the fibre, the radiation was absorbed in its core, leading to laser transitions of the ytterbium. The pump combiner had a (2 + 1) × 1 configuration: two multimode input ports, one single-mode input port and a double-clad single-mode output port. The wavelength of the LDs was ~978 nm, and the highest power of each LD was ~6 W. The single-mode laser radiation propagated along the fibre core. The reflectors of the laser cavity were a wavelength-tunable fibre Bragg grating (TFBG) and a perpendicularly cleaved end facet of the output fibre (Fresnel reflection coefficient of ~4%). In our experiments, we used two TFBGs, with tuning ranges of 1016–1035

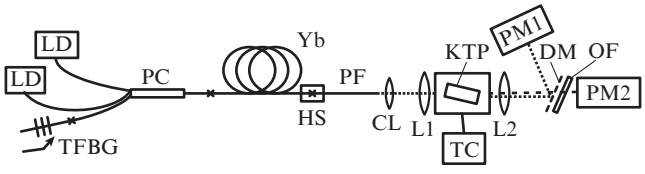

Figure 1. Schematic of the experimental setup for frequency doubling of an ytterbium fibre laser.

* Presented at the Laser Optics Conference, St. Petersburg, Russia, June 2012.

E.I. Dontsova, S.I. Kablukov Institute of Automation and Electrometry, Siberian Branch, Russian Academy of Sciences, prosp. Akad. Koptyuga 1, 630090 Novosibirsk, Russia; e-mail: ekaterina.dontso@mail.ru, kab@iae.nsk.su;
S.A. Babin Institute of Automation and Electrometry, Siberian Branch, Russian Academy of Sciences, prosp. Akad. Koptyuga 1, 630090 Novosibirsk, Russia; Novosibirsk State University, ul. Pirogova 2, 630090 Novosibirsk, Russia; e-mail: babin@iae.nsk.su

Received 24 October 2012; revision received 19 March 2013
Kvantovaya Elektronika **43** (5) 467–471 (2013)
Translated by O.M. Tsarev

Table 1.

Fibre manufacturer and type	Nufern (SM-YDF-5/130)	CorActive I (LAS-Yb-06-02)	CorActive II (DCF-Yb-6/125)
Cladding pump absorption/dB m^{-1} (λ_p = 976 nm)	1.76	2.78	2.47
Inner-cladding diameter/mm	130	127	127
Inner-cladding shape	Octagon	Hexagon	Hexagon
Core diameter/mm	No data	6.6	6.7
Mode field diameter/μm (λ = 1060 nm)	6.5	No data	No data
Effective numerical aperture of the core	0.13	0.13	0.12
Effective numerical aperture of the cladding	0.46	0.47	$\geqslant$0.45

and 1020–1040 nm. The TFBGs were fusion-spliced to the single-mode input port of the coupler. In Fig. 1, the fusion splices of the single-mode fibres are denoted by crosses. A single-clad passive fibre (PF) with a mode field diameter of 6.2 μm was used to outcouple the unabsorbed multimode pump radiation. The fusion splice between the active and passive fibres was covered with gel for outcoupling the unabsorbed pump radiation and placed in a heatsink (HS) for heat removal.

The laser frequency was doubled in a single-pass configuration. The output end face of the fibre laser was located at the focus of a collimating lens (CL). Lens L1 focused the laser output into a KTP nonlinear crystal, which was placed in a thermostat with a temperature controller (TC). The beam emerging from the crystal was collimated by lens L2 and separated by a dichroic mirror (DM) into the fundamental and second harmonics. Their powers were measured by PM1 and PM2 power meters, respectively. The visible light behind the dichroic mirror was further filtered by an optical filter (OF).

The TFBGs were tuned via axial compression in a mount. Compression of a fibre Bragg grating changes its period and effective refractive index, leading to changes in Bragg resonance wavelength and, hence, in laser wavelength. The grating design and tuning mechanism were described in detail elsewhere [5].

The gain media of the laser were Nufern and CorActive standard active fibres. The main characteristics of the fibres are listed in Table 1.

In our experiments, we used a 0.73-m length of CorActive I (CA I) fibre, 1.3-m length of CorActive II (CA II) and 1.85- and 2.75-m lengths of Nufern (N) fibre. Figure 2 shows the output power P_{las} as a function of laser wavelength λ_{las} for the active fibres used. The total power of the two laser diodes measured behind the pump combiner was 11.5 W in the experiments with CA II and 11.1 W in the experiments with the other fibres.

Figure 3 shows tunable laser spectra of the 1.85-m-long N fibre. It is seen that tuning to shorter wavelengths leads to an increase in spontaneous emission near the gain maximum at about 1035 nm, to the point of chaotic lasing, which 'takes away' some of the pump energy and reduces the output power at the fundamental frequency. The drop in power is especially marked at the short-wavelength edge of the tuning curve (Fig. 2) because parasitic lasing occurs even at the end point of the curve (1020.3 nm for the 1.85-m-long N fibre).

Figure 4 presents a stable emission spectrum of a CA I fibre laser (λ = 1018.9 nm) near the short-wavelength limit of its tuning range. It follows from the spectra in Figs 3 and 4 that the difference between the power of the fundamental signal and the power at the spontaneous emission maximum

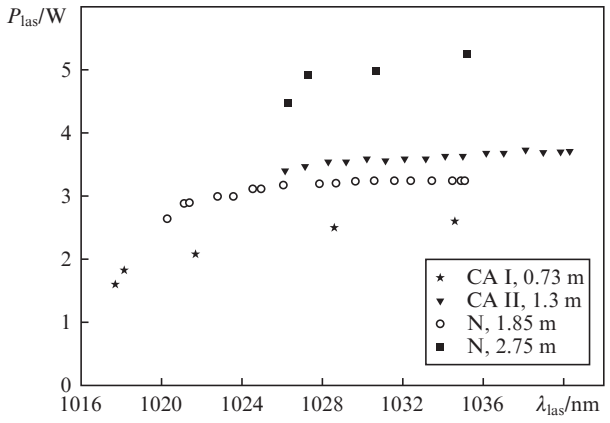

Figure 2. Laser output power and wavelengths for different active fibres in the laser cavity.

before chaotic lasing development is 50 dB for the 1.85-m-long N fibre and 40 dB for the CA I fibre.

The highest laser output power (at least 5 W) was obtained with the 2.75-m-long N fibre, but we failed to tune it to considerably shorter wavelengths because extra peaks emerged in its output spectrum near 1035–1040 nm.

The laser output power was found to drop at the shortest wavelength for all the active fibres (Fig. 2). Extra peaks in the laser output spectrum were observed for the 1.85- and 2.75-m

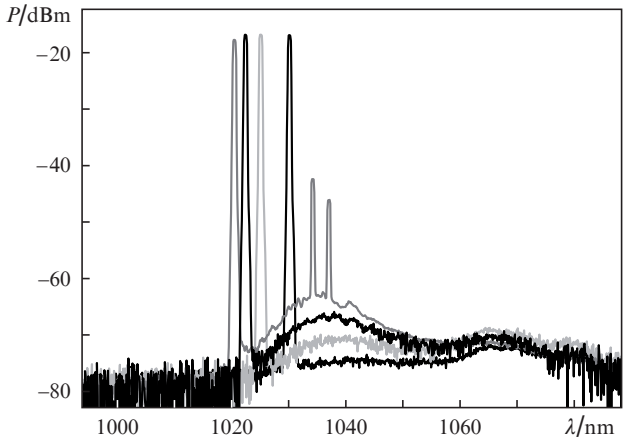

Figure 3. Laser output spectra for tuning to shorter wavelengths relative to the gain maximum of the 1.85-m-long N fibre (laser emission lines at 1030, 1025, 1022.3 and 1020.3 nm).

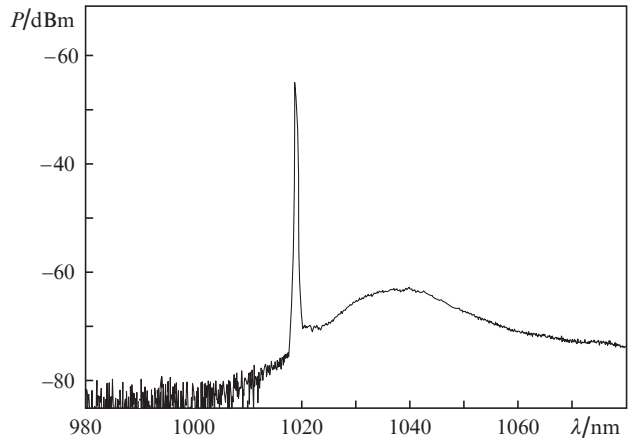

Figure 4. Output spectrum of an ytterbium fibre laser operating at 1018.9 nm.

N and CA I fibres. No detailed spectral measurements were made for CA II, but extra peaks were detected. It is worth noting that tuning to longer wavelengths was only limited by the parameters of the grating used.

3. Laser power calculation

To analyse the experimental data obtained, we used a model [6] in which the output power of a fibre laser, P_{las}, at a pump power P_p^{in} is

$$P_{las} = \eta(P_p^{in} - P_p^{th}), \tag{1}$$

where

$$P_p^{th} = h\nu P_s^{cs}[\alpha_s L - \ln(\varepsilon R)][1 - (G_{max}\varepsilon R)^{-\delta}]^{-1}$$

is the lasing threshold;

$$\eta = \eta_q \varepsilon_2 (1 - R_2)\, T_{eff}^{-1}[1 - (G_{max}\varepsilon R)^{-\delta}] \tag{2}$$

is the slope efficiency;

$$G_{max} = \exp[(\alpha_p/\delta - \alpha_s)L] \tag{3}$$

is the maximum gain; L is the length of the gain medium; P_s^{cs} is the saturation power of the signal wave; $\alpha_{p,s}$ are the absorption coefficients for the pump and signal waves; δ is the ratio of the saturation powers of these waves; η_q is quantum efficiency; h is the Planck constant; ν is the frequency of the light;

$$T_{eff} = (1 - \varepsilon_2^2 R_2) + [(1 - \varepsilon_1^2 R_1)\varepsilon_2^2 R_2]/(\varepsilon R)$$

is the effective transmission loss coefficient; R_1 and R_2 are the reflectances of the cavity input and output mirrors; ε_1, ε_2 are the transmittances of the fusion splices; $\varepsilon = \varepsilon_1\varepsilon_2$; and $R = \sqrt{R_1 R_2}$.

In our calculations, we used the experimentally determined values $\varepsilon_1 = \varepsilon_2 = 0.85$ (~15% loss in the fusion splice to the active fibre) and $\delta = 0.016$ (for the CA I and CA II fibres) and 0.013 (for N).

The absorption cross sections for the pump and signal waves, σ_{pa} and σ_{sa} are related to the absorption coefficients by

$$\alpha_p = \Gamma_p N\sigma_{pa} \text{ and } \alpha_s = \Gamma_s N\sigma_{sa},$$

where Γ_p and Γ_s are the overlap integrals and N is the ion concentration in the cross section of the fibre core.

Consider in greater detail Eqn (2) at small L and R_2. In our case, $R_2 = 0.04$, $\varepsilon R = 0.142$ and, hence, $(\varepsilon R)^{-\delta}$ is close to unity. So it is omitted in what follows and we have $T_{eff} \approx 1$. The value of $\alpha_p L$ does not exceed 1.5, and the $\alpha_s \delta L$ product increases with decreasing wavelength because of the increase in σ_{sa} [1, 7]. Given the above, we obtain

$$\eta \approx \eta_q \varepsilon_2 (1 - R_2)(\alpha_p - \alpha_s \delta)L. \tag{4}$$

Well above the lasing threshold, we have

$$P_{las} \approx \eta P_p^{in}. \tag{5}$$

The calculated and observed responses of the output power of the fibre lasers to wavelength tuning are illustrated in Fig. 5, where the solid and dot-dot-dashed lines represent calculations for $P_{th} = 0$ and $P_{th} \neq 0$, respectively. The value of η was calculated using Eqn (2). It is seen that taking into account the threshold pump power has no significant effect on the behaviour of P_{las} and cannot explain the short-wavelength drop in output power. When the simplified formula (4) was used, the η of the CA I fibre laser (dashed line) was overestimated by ~25%.

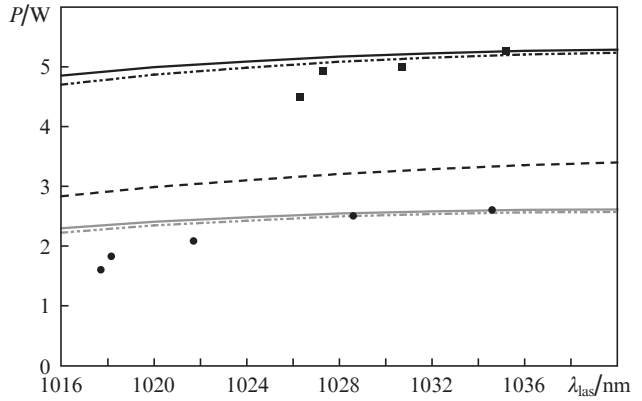

Figure 5. Measured laser output powers for the CA I (●) and 2.75-m-long N (■) fibres, corresponding calculation results with (dot-dot-dashed lines) and without (solid lines) allowance for the threshold pump power and results obtained using a simplified formula for η (dashed line).

In our experiments, reducing the laser wavelength leads to a drop in output power because of the increase in α_s and the associated decrease in η in (4). Moreover, the spontaneous emission intensity in the range 1040–1050 nm increases, leading to ever higher absorbed energy losses. The last effect is left out of consideration in the above model. Nevertheless, the model allows one to rather accurately evaluate the laser output power when the laser wavelength is tuned in the range where the gain band is effectively saturated and, hence, the contribution of amplified spontaneous emission is small.

4. Second-harmonic generation

The frequency of a cw ytterbium fibre laser was doubled using an 18-mm-long KTP crystal with type II phase matching

(oe→e) in the XY plane, optimised for operation near 1030 nm. The choice of the crystal geometry was dictated by the requirement to minimise the walk-off of the extraordinary wave by using oblique incidence of the beam on the crystal [8]. The laser second-harmonic generation efficiency depends on the walk-off angle at the fundamental frequency [9].

At a given angle of incidence of light, ϑ, on a crystal with a cut angle ζ (which is determined by the directions of the crystallographic axis X of the crystal and the normal to its surface), one can evaluate the phase matching wavelength and the walk-off angle of the fundamental harmonic, ψ. Varying the ϑ angle, one can find conditions that ensure walk-off compensation for the extraordinary wave at oblique incidence. In our experiments, we used a crystal with a cut angle $\zeta = 53.5°$. Figure 6a shows the angle of incidence as a function of phase matching wavelength, and Fig. 6b presents the calculated walk-off angle as a function of phase matching wavelength. At zero crossing, the compensation condition for the walk-off angle of the extraordinary wave, β, is fulfilled and the fundamental beams completely coincide ($\psi = 0$). In our case, this condition is fulfilled at a wavelength of 1031 nm. (In the calculations, we used dispersion relations for refractive indices [10].)

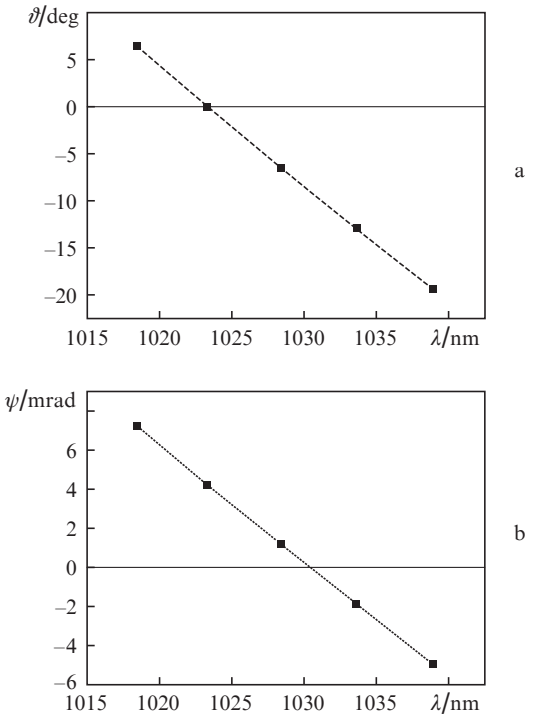

Figure 6. (a) Phase matching wavelength at different angles of incidence of light on a crystal and (b) spectral dependence of the walk-off angle for a crystal with $\zeta = 53.5°$.

The total effective nonlinearity coefficient for second-harmonic generation ($\gamma = P_{2\omega}/P_{\omega}^2$) was measured as a function of wavelength in the tuning range 1020–1040 nm. The second-harmonic power was found to depend significantly on laser wavelength (Fig. 7), whereas the fundamental harmonic power remained essentially unchanged.

As seen in Fig. 7, the effective nonlinearity coefficient for second-harmonic generation has a maximum ($\sim 1.4\times10^{-3}$ W^{-1}) at ~1031 nm. This wavelength coincides with that evaluated from the walk-off compensation condition for our crystal (Fig. 6b).

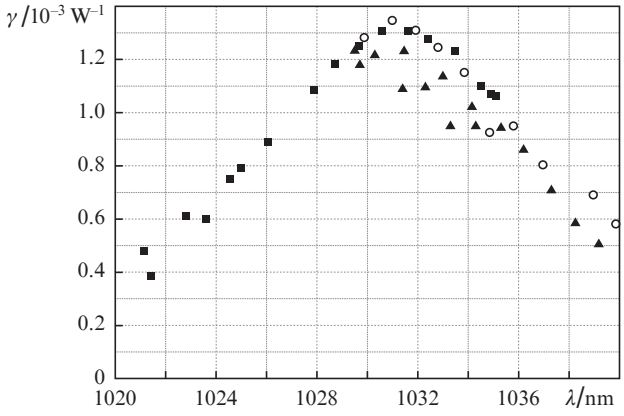

Figure 7. Total effective nonlinearity coefficient of second-harmonic generation for lasers based on the 1.85-m-long N fibre (■, ▲) and CA II fibre (○) with the use of tunable Bragg gratings.

In a previous study [11], frequency doubling of a tunable fibre laser in a 8-mm-long KTP crystal in the XY plane was analysed near a laser wavelength of 1070 nm. Efficient frequency doubling was achieved at angles of incidence corresponding to small ψ angles. In addition, it was proposed that the possible tuning range could be assessed using a graph of ψ against λ. The tuning range where efficient frequency doubling took place was 1062–1078 nm, and the angle ψ was within 9 mrad [11]. In this study, the half-maximum second-harmonic generation (SHG) range of the 18-mm-long crystal

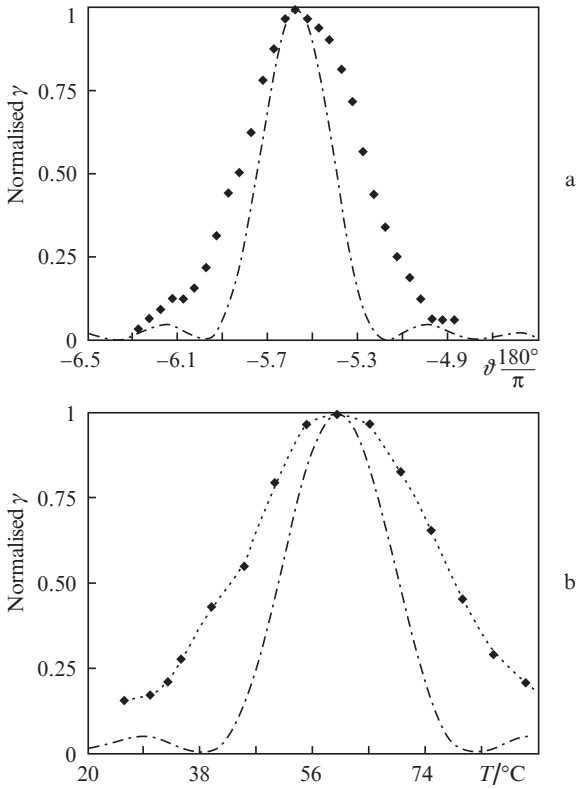

Figure 8. Total effective nonlinearity coefficient of second-harmonic generation as a function of the (a) angle of incidence and (b) crystal temperature.

is 1024–1037 nm and the walk-off angle is within 4 mrad, i.e. half that in the crystal about half as long.

The experimentally determined spectral width of the phase matching region is ~0.5 nm, whereas the calculated one is 0.3 nm. The discrepancy may result from the rather large laser emission bandwidth (~0.1 nm), which was measured by a Yokogawa AQ6370 optical spectrum analyser with a 0.02-nm resolution. The visible emission bandwidth for single-pass frequency doubling was ~40 pm [the spectrum was measured by an LSA spectrum analyser (Angstrom HighFinesse)]. Thus, the width of the second-harmonic spectrum was about half that of the fundamental, which was equivalent to a factor of 2 increase in the width of the frequency spectrum. As shown earlier [12], in the SHG process the width of the frequency spectrum depends on its shape and radiation statistics. If radiation has a random character, the spectrum is about twice as broad. It is such character of phases of an ytterbium-doped fibre laser with Bragg gratings that was demonstrated by Kablukov et al. [13].

Figure 8 shows the calculated and measured total effective SHG nonlinearity coefficients as functions of the angle of incidence and crystal temperature. It follows from Fig. 8 that the measured width of the phase matching curves also exceeds the calculated one. The discrepancy is caused by several factors: the broadening of the phase matching curve may be due not only to the large laser emission bandwidth but also to sharp radiation focusing [9] and inhomogeneities in the structure of the crystal, which reduce the frequency doubling efficiency.

5. Main results

We have studied output characteristics of a diode-cladding-pumped ytterbium-doped fibre laser. The use of a tunable fibre Bragg grating allowed us to tune the laser wavelength from 1040 to 1017 nm in an all-fibre configuration. The laser efficiency was at least 45% in the range 1027–1040 nm and at least 27% in the range 1021–1035 nm. The 1020-nm efficiency of a laser made using CorActive fibre was 19%, which is about a factor of 3 lower than that of lasers that are pumped by high-power diodes and employ specialty fibres with a small ratio of the inner-cladding and core diameters [1, 2].

We have demonstrated and investigated SHG in a KTP crystal, tunable in a wide spectral range (509–520 nm). For frequency doubling in optimised KTP geometry, we have examined the total effective nonlinearity coefficient as a function of laser wavelength (γ was maximal, 1.4×10^{-3} W^{-1}, at λ = 1031 nm at an almost constant fundamental harmonic power throughout the tuning range). The maximum second-harmonic power at ~515 nm was 15 mW in a single-pass configuration. The tunable visible light source obtained can be used in Raman spectroscopy, flow cytometry, confocal microscopy and other biomedical applications, where power levels in the range 10–100 mW are typically sufficient.

Acknowledgements. This work was supported by the RF Ministry of Education and Science, the Physical Sciences Division of the Russian Academy of Sciences (RAS) and the Siberian Branch of the RAS (integrated research project).

References

1. Kurkov A.S., Dianov E.M. *Kvantovaya Elektron.*, **34**, 881 (2004) [*Quantum Electron.*, **34**, 881 (2004)].
2. Kurkov A.S. *Laser Phys. Lett.*, **4** (2), 93 (2007).
3. Kurkov A., Medvedkov O.I., Paramonov V.M., Vasiliev S.A., Dianov E.M., Solodovnikov V. *Proc. Conf. Optical Amplifiers and Their Applications* (Stresa, Italy, OSA, 2001) paper OWC2.
4. Kablukov S.I., Dontsova E.I., Akulov V.A., Vlasov A.A., Babin S.A. *Laser Phys.*, **20** (2), 360 (2010).
5. Babin S.A., Kablukov S.I., Vlasov A.A. *Laser Phys.*, **17** (11), 1323 (2007).
6. Barnard C., Myslinski P., Chrostowski J., Kavehrad M. *IEEE J. Quantum Electron.*, **30** (8), 1817 (1994).
7. Mel'kumov M.A., Bufetov I.A., Kravtsov K.S., Shubin A.V., Dianov E.M. *Preprint, 5* (Moscow: Nauchn. Tsentr Volokonnoi Optiki Inst. Obshchei Fiziki Ross. Akad. Nauk, 2004) p. 57.
8. Asaumi K. *Appl. Opt.*, **37** (3), 555 (1998).
9. Dmitriev V.G., Tarasov L.V. *Prikladnaya nelineinaya optika* (Applied Nonlinear Optics) (Moscow: Radio i Svyaz', 1982) p. 350.
10. Kato K., Takaoka E. *Appl. Opt.*, **41** (24), 5040 (2002).
11. Akulov A.V., Kablukov S.I., Babin S.A. *Kvantovaya Elektron.*, **42** (2), 120 (2012) [*Quantum Electron.*, **42** (2), 120 (2012)].
12. Akhmanov S.A., D'yakov Yu.E., Chirkin A.S. *Vvedenie v statisticheskuyu radiofiziku i optiku* (Introduction to Statistical Radiophysics and Optics) (Moscow: Nauka, 1981) p. 640.
13. Kablukov S.I., Zlobina E.A., Podivilov E.V., Babin S.A. *Opt. Lett.*, **37** (13), 2508 (2012).